Ultrasonics 116 (2021) 106495

Contents lists available at ScienceDirect

Ultrasonics

journal homepage: www.elsevier.com/locate/ultras

Development and validation of low-intensity pulsed ultrasound systems for highly controlled *in vitro* cell stimulation

F. Fontana [a,b], F. Iberite [a,b], A. Cafarelli [a,b], A. Aliperta [a,b], G. Baldi [a,b], E. Gabusi [c], P. Dolzani [c], S. Cristino [d], G. Lisignoli [c], T. Pratellesi [e], E. Dumont [f], L. Ricotti [a,b]

[a] The BioRobotics Institute, Scuola Superiore Sant'Anna, 56127 Pisa, Italy
[b] Department of Excellence in Robotics & AI, Scuola Superiore Sant'Anna, 56127 Pisa, Italy
[c] IRCCS Istituto Ortopedico Rizzoli, SC Laboratorio di Immunoreumatologia e Rigenerazione Tissutale, 40136 Bologna, Italy
[d] Dipartimento Scienze Biologiche, Geologiche e Ambientali (BiGeA), Università di Bologna, 40126 Bologna, Italy
[e] BAC Technology s.r.l., 50063 Florence, Italy
[f] Image Guided Therapy, 33600 Pessac, France

ARTICLE INFO

Keywords:
Biophysical stimulation
Cell stimulation
LIPUS
Ultrasound
In vitro set-up

ABSTRACT

This work aims to describe the development and validation of two low-intensity pulsed ultrasound stimulation systems able to control the dose delivered to the biological target. Transducer characterization was performed in terms of pressure field shape and intensity, for a high-frequency range (500 kHz to 5 MHz) and for a low-frequency value (38 kHz). This allowed defining the distance, on the beam axis, at which biological samples should be placed during stimulation and to exactly know the intensity at the target. Carefully designed retaining systems were developed, for hosting biological samples. Sealing tests proved their impermeability to external contaminants. The assembly/de-assembly time of the systems resulted ~3 min. Time-domain acoustic simulations allowed to precisely estimate the ultrasound beam within the biological sample chamber, thus enabling the possibility to precisely control the pressure to be transmitted to the biological target, by modulating the transducer's input voltage. Biological *in vitro* tests were also carried out, demonstrating the sterility of the system and the absence of toxic and inflammatory effects on growing cells after multiple immersions in water, over seven days.

1. Introduction

Ultrasound (US) is a physical tool widely used for medical diagnoses, as well as for therapeutic purposes in surgery, ophthalmology and physiotherapy [1]. In addition to its low-cost and its intrinsic safety, US is gaining importance because it can be remotely delivered to the target area in a non-invasive manner, thus bringing a therapeutic action inside the body, without any scar.

Two main US-related physical effects can be exploited: thermal and mechanical ones [2]. Typically, high-intensity US is based on thermal effects, as in the case of high intensity focused US. Here, the absorption of ultrasonic energy and heat production can be used for hyperthermia or tissue ablation [3]. Differently, at lower intensity (0.5 to 3000 mW/cm^2) [4], US results in mechanical effects only, with small or null temperature increase. This is often exploited for reparative/regenerative treatments [5]. The application of therapeutic US involves the choice of several parameters: frequency, intensity, duration of the treatment, duty-cycle, etc. The frequency value that is typically adopted for physiotherapy is 1 MHz, which can reach up to 3 MHz in some commercial equipment [6]. These conditions are also the ones typically employed for *in vitro* experiments, with results that are promising, although in many cases not coherent or even contradictory, among different studies [7–9]. Some attempts were recently made to broaden this range [10,11] moving to the low-frequencies domain, which may have advantages with respect to high-frequency US, such as anti-inflammatory effects, bactericide action, effects on the vascular and epithelial permeability, etc. [12–14].

Low-intensity pulsed ultrasound (LIPUS) is a specific US modality

E-mail addresses: fr.fontana@santannapisa.it (F. Fontana), federica.iberite@santannapisa.it (F. Iberite), andrea.cafarelli@santannapisa.it (A. Cafarelli), andrea.aliperta@santannapisa.it (A. Aliperta), gabriele.baldi@santannapisa.it (G. Baldi), elena.gabusi@ior.it (E. Gabusi), paolo.dolzani@ior.it (P. Dolzani), sandra.cristino@unibo.it (S. Cristino), gina.lisignoli@ior.it (G. Lisignoli), tiziano.pratellesi@gmail.com (T. Pratellesi), erik.dumont@imageguidedtherapy.com (E. Dumont), leonardo.ricotti@santannapisa.it (L. Ricotti).

https://doi.org/10.1016/j.ultras.2021.106495
Received 20 October 2020; Received in revised form 25 April 2021; Accepted 2 June 2021
Available online 15 June 2021

relying on low-intensity pulsed waves. It has been approved by the Food and Drug administration (FDA) as a means to promote bone fracture healing [15]. Furthermore, it has been proved to promote chondrocyte proliferation and survival, to accelerate bone maturation and callus formation [16], to promote nerve regeneration [7] to allow neuromodulation [17] and other medical applications. However, a better understanding of the interaction mechanisms between US waves and cells is still needed, to allow LIPUS therapeutic procedures to be defined as entirely safe, highly controlled and repeatable.

Surprisingly, very few studies report *in vitro* results derived from highly controlled US exposure systems, able to carefully regulate and quantify the pressure applied to the biological target. Indeed, in many studies researchers adopt LIPUS systems that are prone to errors both during calibration and use. As a result, the actual US dose delivered to cells can be up to 700% larger or smaller than the expected one, due to physical phenomena like attenuation, reflection, diffraction, standing waves generation and scattering [18,19]. This is an important issue that hampers the achievement of reliable *in vitro* results and slows down the future clinical translation of LIPUS treatments.

The first source of possible errors consists of a lack of appropriate US transducer characterization: very often, researchers are not aware of the precise pressure map and the relationship between the driving voltage and pressure amplitude at the target, for the transducers employed.

The second source of possible errors concerns the overall set-up configuration. Alassaf et al. [20] and Snehota el al. [21] classified the set-ups typically used for *in vitro* US stimulations in three main categories: (a) systems in which the US transducer is positioned directly below a culture well containing cells, and an acoustic gel is used to couple between the transducer and the well (the well and the transducer are not immersed in water); (b) systems in which the US transducer is directly immersed in the well medium; (c) systems in which water is used to couple between the transducer and the sample, both immersed in the liquid media.

Concerning point (a), the main problem affecting this kind of set-ups is the negletion of reflection phenomena. Samples are exposed to air in the external environment, even if acoustically coupled to the transducers in a proper way. Thus, wave reflection occurs due to acoustic impedance differences, unavoidably altering experimental conditions. Furthermore, samples are usually retained in traditional multi-well plates, which disturb the correct transmission of mechanical waves. It is well known that the transmission and reflection coefficients of ultrasonic waves passing through a layer are frequency-dependent [22]. The transmission coefficient has its maximum value and the reflection coefficient has its minimum value when the thickness of the layer is at least smaller than a quarter of the wavelength [23]. This phenomenon should be carefully considered to guarantee a fully controlled stimulation.

Ventre et al. [24] adopted the same configuration mentioned in point (a), but substituting gel coupling with degassed water, only partially immersing samples in it. Also in this case, as well as for set-ups falling into the (b) category, reflections due to the air interface still bring a source of errors, due for example to an unpredictable generation of standing waves.

Systems falling into the (c) category aim to minimize reflection phenomena. An example of this kind of set-up was reported by Salgarella et al. [10]. Here the authors used a linear rail to allow movement of the sample along the beam axis of the transducer, to enable alignment of the cells at the location of the axial maximum of the generated pressure field. Furthermore, they adopted a US-transparent cell culture well, based on a multilayered structure, designed to provide cell cultures with controlled US amplitudes. It consisted of a thin (25 μm) polystyrene film, secured within a polytetrafluoroethylene cylindrical well that contained cell culture medium. A secure mounting of the structure was guaranteed through a custom 3D printed cup. However, such a custom well was not tested in terms of full sealing ability and sterility overtime and implied an elaborated manipulation of its components by the user, with a long time needed to perform a single stimulation task, a high risk of contamination and a consequent difficulty in carrying out long-term experiments. A different approach was proposed by Zhao et al. [25], with the Opticell™ chamber used as a cell culture system seeded with cells and filled with culture medium. However, parallel-plate chambers are affected by some drawbacks, such as the occurrence of shear stresses during liquid injection and the difficulty in removing air bubbles entrapped in the system, that can compromise the delivery of a reliable US amplitude.

Driven by these considerations, the aim of this work is to describe two *in vitro* highly controlled LIPUS stimulation systems able to deliver a precise US beam to the biological target. They allow exploring US stimulation in a wide range of frequencies and intensities and can guarantee at the same time ease of use and full sterility of the tested samples, paving the way to fully controlled and reliable *in vitro* experiments.

2. Development of the LIPUS set-ups

2.1. Overall architecture of the systems

Two LIPUS systems were developed for low and high frequency cell stimulation.

The low-frequency set-up is shown in Fig. 1a, b. It consisted of: a tank ($200 \times 200 \times 350$ mm^3) filled with deionized and degassed water; an upper acoustic absorber (a pyramidal-shaped material, able to prevent acoustic reflections along the acoustic path– Aptflex F28P, Precision Acoustics, Dorchester, Dorset, UK), positioned above the stimulated biological samples; a lateral acoustic absorber, able to absorb possible horizontally-deviated waves (Aptflex F28, Precision Acoustics, Dorchester, Dorset, UK); a biological sample-retaining system, designed to be water-proof and as much as possible transparent to US, equipped with one chamber, positioned at a fixed distance from the transducer and coaxial with it; a 50 mm diameter US transducer (BAC s.r.l., Florence, Italy), able to provide a 38 kHz stimulation (approximately 4 cm wavelength), and fixed at the bottom of the tank; an exhaust valve, to empty and fill the tank; a signal generator (BAC s.r.l., Florence, Italy), to control the electric input signal to the transducer (2 W maximum power, with the possibility to vary treatment duration, duty-cycle, pulse repetition frequency, voltage amplitude through a touch-screen platform); and a degassing system (IGT, Bordeaux, France), which includes a vacuum pumped membrane contactor (3M™ Liqui-Cel™, St Paul, Minnesota, USA), to degas water within the tank.

In Fig. 1c, d, the high frequency set-up is shown, together with its components: a tank ($265 \times 245 \times 490$ mm^3) filled with deionized and degassed water; an upper acoustic absorber, similar to the previously described one; a biological sample retaining system, water-proof and transparent to US, equipped with three chambers, connected to a linear rail in order to allow its translation on the z-axis and thus modify its distance from the transducer; three transducers (Precision Acoustics, Dorchester, Dorset, UK), fixed at the bottom of the tank, which produce high-frequency (500 kHz to 5 MHz) ultrasonic waves ; an exhaust valve, to empty and fill the tank; a multichannel signal generator (IGT, Bordeaux, France), to control the electric input signal to the transducer (2 W maximum power per channel, with the possibility to vary treatment duration, duty-cycle, pulse repetition frequency, voltage amplitude); and the same degassing system previously described. In order to cover the broad frequency range from 500 kHz to 5 MHz, five different types of unfocused transducers were used: three 44 mm diameter transducers, centered on 0.6 MHz and used, in this study, at 500 and 750 kHz; three 23 mm diameter transducers, centered on 1 MHz; three 23 mm diameter transducers, centered on 2 MHz; three 15 mm diameter transducers, centered on 3 MHz; three 15 mm diameter transducers, centered on 4 MHz and used, in this study, at 4 and 5 MHz, for a total of 15 transducers employed in the high-frequency range.

The multichannel signal generator was based on highly linear amplifiers (class A/B), able to generate pure sinusoidal signals avoiding

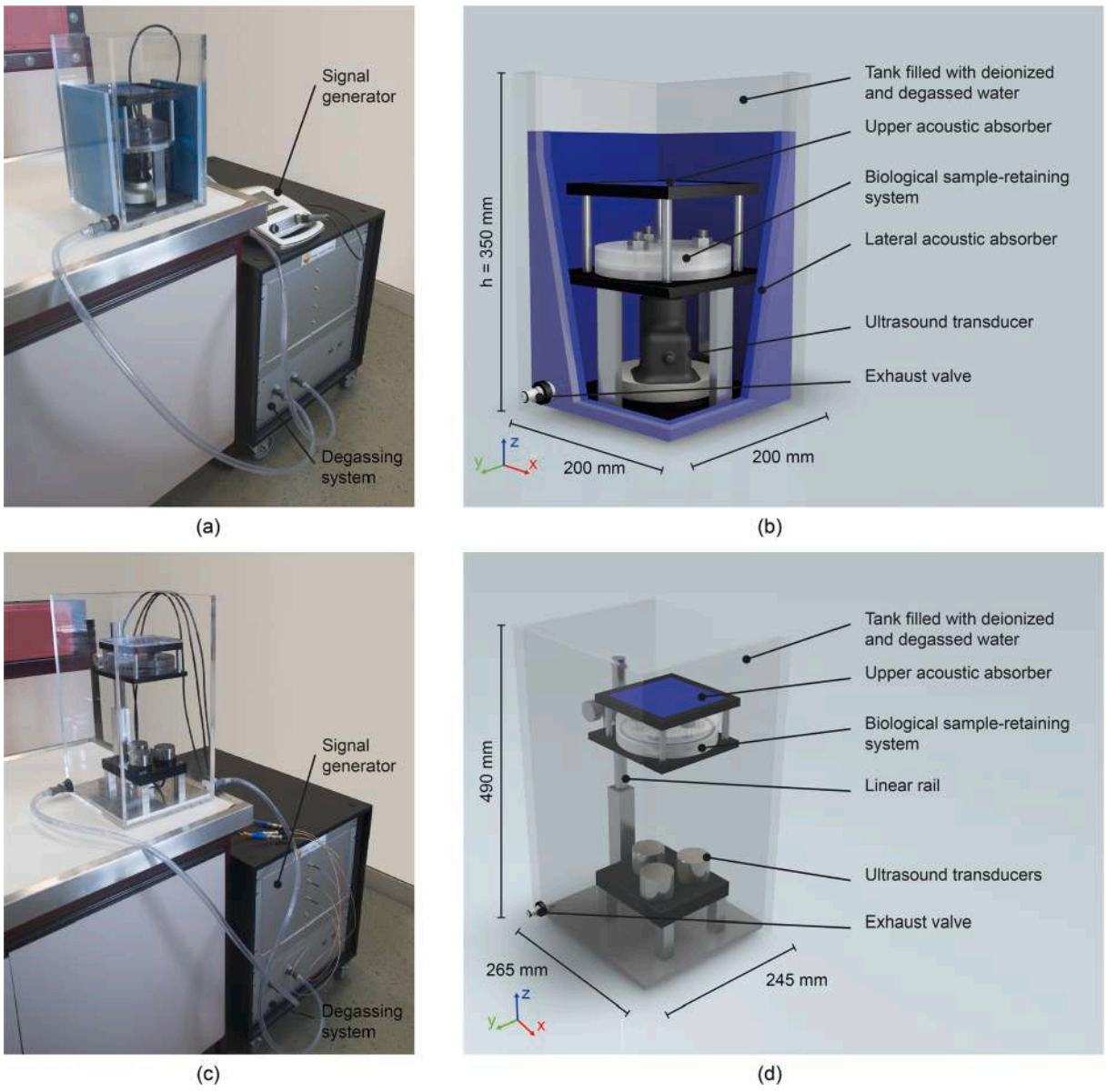

Fig. 1. LIPUS system for low frequency and high frequency cell stimulation: (a) Overall view of the low frequency system; (b) Rendered CAD of the low frequency system; (c) Overall view of the high frequency system; (d) Rendered CAD of the high frequency system.

harmonics contamination of the produced US. Furthermore, stimulation parameters for this generator were easily tunable thanks to a dedicated software, based on a user-friendly graphical user interface (shown in Fig. S1).

2.2. Characterization of US transducers

Normalized pressure field shape, produced by the transducer working at 38 kHz, was measured adopting a calibration system already described by the authors [26] (Fig. S2) and equipped with a hydrophone (Precision Acoustics, Dorchester, Dorset, UK – 2 mm needle; mean sensitivity in the range 0.1 MHz to 10 MHz: 3.5 V/MPa; typical frequency response: flat (4 dB) over the range 100 kHz to 10 MHz). The same experimental procedure was used for five types of transducers working at seven stimulation frequencies in the range 500 kHz−5 MHz. Pressure field maps are shown in Fig. 2a, in terms of normalized peak-to-peak pressure.

The generated acoustic fields were also simulated in free-field conditions with the k-Wave Matlab open-source toolbox [27,28]. The simulated beams are shown in Fig. 2b and resulted qualitatively similar to the direct measurements. A quantitative comparison (see Fig. S3) also demonstrated a good agreement between the measured beams and the simulated ones. The small mismatch between the two beams groups was probably due to almost unavoidable errors in the measurements.

The horizontal dashed red lines in Fig. 2 highlight the distances, on the z-axis, at which biological samples should be placed during stimulation (corresponding to a far-field condition, in which the ultrasonic field is fully formed and is homogeneous, as it can be observed from the pressure maps).

For the intensity calibration at 38 kHz, an omnidirectional hydrophone Reson TC 4034, with a frequency response from 1 Hz to 470 kHz (±3 dB), was used. Results are shown in Fig. 3a, as input peak-to-peak pressure read by the hydrophone positioned along the axial direction of the transducer at a specific distance, against the voltage provided by the generator to the 38 kHz transducer. Measurements were taken, at a distance corresponding to the dashed line shown in Fig. 2a.

For the transducers working in the frequency range 500 kHz−5 MHz, the intensity was measured using the same system adopted for pressure

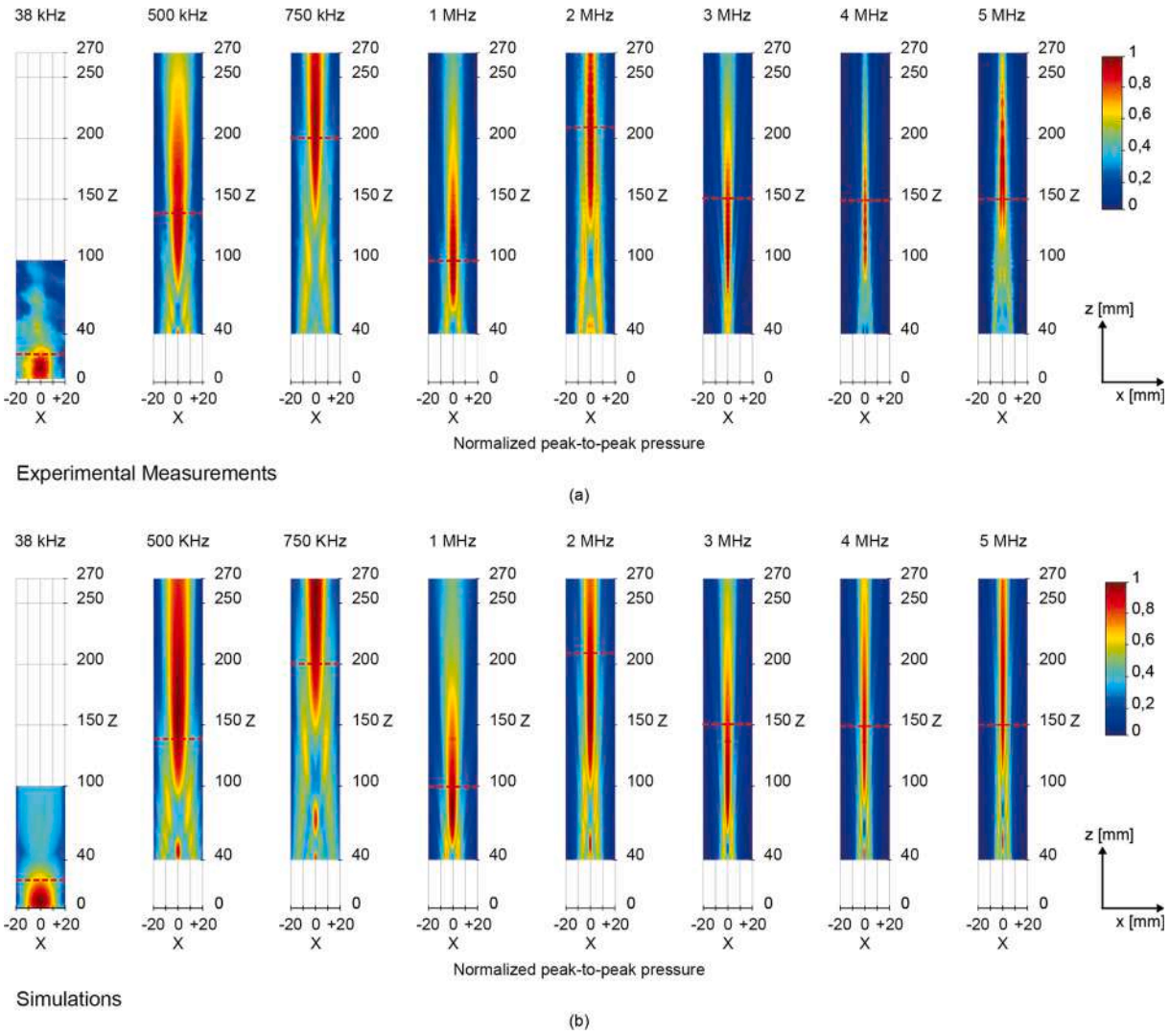

Fig. 2. Experimental measurements (a) and simulated beams (b) obtained for transducers working in the frequency range 38 kHz−5 MHz.

field shape characterization. In Fig. 3b, representative curves are shown for the 1 MHz frequency case: the behavior of three different transducers, working at the same frequency, is presented (as visible in Fig. 1c, d, all the three transducers can be integrated into the system, to guarantee the stimulation of three different biological samples at the same time). The peak-to-peak pressure was evaluated, with respect to the previously shown pressure fields, in correspondence to the dashed lines along the z-axis. Similar curves were obtained for the other transducers, as shown in Fig. S4.

2.3. Biological sample-retaining system

The retaining system is a key element of the platforms. It hosts biological samples during LIPUS stimulations. Such stimulations must be necessarily carried out in deionized and degassed water to guarantee a highly controlled US wave transmission, without attenuations and reflections. For this reason, the retaining system must fulfill two fundamental requirements: on the one hand, it must guarantee full transparency to US waves (i.e., must prevent undesired reflections and attenuations, so as to control the pressure amplitude); on the other hand, it must guarantee the sterility of the samples that undergo stimulation. This means that they must be kept isolated from the external environment, avoiding water penetration within biological wells.

Single-well and triple-well retaining systems (named LFS and HFS, respectively) were designed for the low frequency and the high-frequency set-ups, respectively. The HFS allows the simultaneous US stimulation of up to three biological replicates at the same time. This facilitates carrying out biological experiments. In Fig. 4a, b, a picture for each retaining system is reported, whereas in Fig. 4c a detail of the biological sample chamber is shown.

Both devices were produced in polycarbonate, to make them biocompatible and autoclavable. At the bottom of the chamber, a latex film was mounted. Such film had a thickness of 60 μm, which is smaller than a quarter of the minimum US wavelength used (i.e., 300 μm at 5 MHz). This condition guarantees transparency of the latex film to the US waves. Then, elastomeric O-rings were positioned to guarantee a hydraulic sealing of the chamber content. A distance of 7 cm was chosen between the center of each retaining chamber of the HFS, to prevent possible overlaps between pressure fields produced by different transducers. The same consideration, regarding the far-reaching ultrasonic waves, led the authors to adopt a single chamber design for the low-frequency retaining system. The open diameter of the retaining chamber was 16 mm for both the LFS and the HFS, while its open height was 18 mm.

Screws and bolts were used to effectively seal the system, in a sterile cabinet (Fig. S6).

Two supplementary videos show an animation of the exploded structure assembly and a video of the mounting procedure of the system

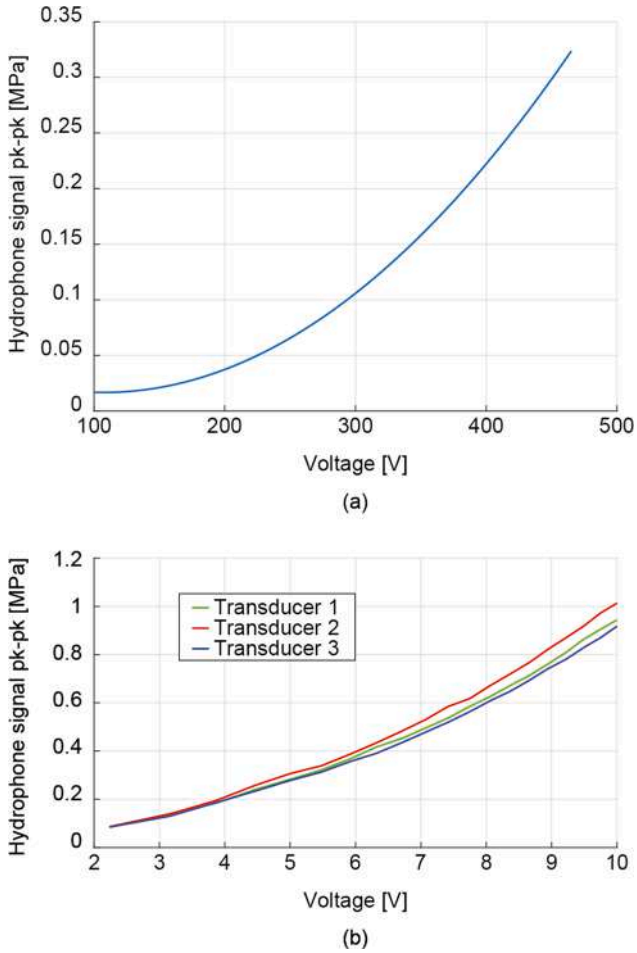

Fig. 3. Peak-to-peak pressure measurement results, as a function of the output voltage provided by the generator for (a) the 38 kHz transducer and (b) the three 1 MHz transducers.

in the cabinet (movie S1 and movie S2, respectively). The above-described solution has been protected through a patent application [29].

The impermeability of the biological sample-retaining systems to external contaminants was assessed through the experiment illustrated in Fig. 5a. The goal of this test was to verify that the chamber content was not contaminated by fluorescein, externally surrounding the system.

Each retaining system chamber was filled with deionized water, assembled and closed. Then the entire system was immersed in a tank and filled with a solution of deionized water and fluorescein sodic salt (a fluorescent molecule) at a concentration of 200 μg/mL. During the sealing experiment, the tank was kept at 37 °C and 1 atm, with the biological sample-retaining system positioned at 7 cm from the liquid surface, for 30 min (these conditions well mimicked the ones to be used in future cell stimulation experiments). Finally, the retaining system was removed from the tank and the fluorescence intensity of the three chambers content was analyzed through a VICTOR Multilabel Plate Reader (PerkinElmer, Waltham, MA, USA). Twelve independent samples were analyzed per each condition.

Impermeability test results are reported in Fig. 5b, c as boxes with 5th to 95th percentiles and median values. The upper and lower whiskers represent the minimum and the maximum values, respectively. "OUT" represents the fluorescence measurement for the solution external to the system (deionized water + 200 μg/mL fluorescein), "IN" represents the fluorescence readout for the chamber content after the sealing test (30 min of incubation), while "H_2O" represents the fluorescence emitted by deionized water without fluorescein, used as the negative control. A Mann-Whitney test ($\alpha = 0.05$) (Graphpad Prism 7)

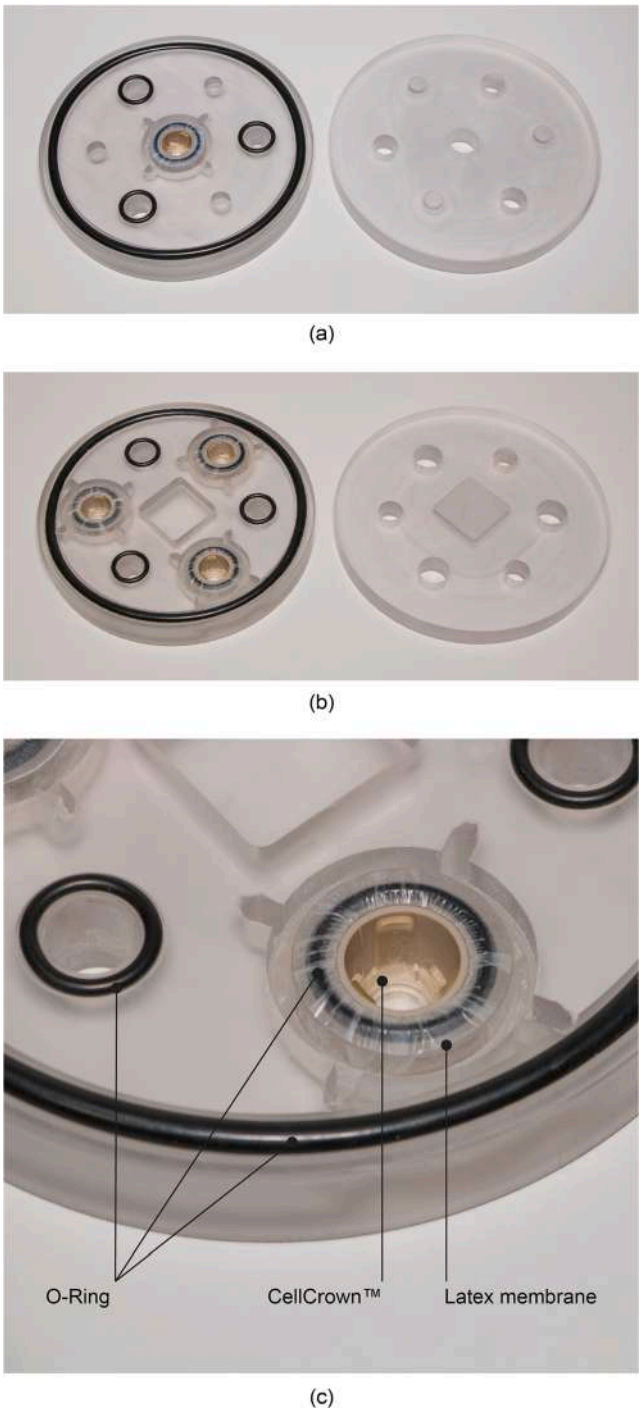

Fig. 4. (a) Picture of the single-well retaining system (LFS); (b) picture of the triple-well retaining system (HFS); (c) retaining chamber detail.

was used to compare the samples. The fluorescence value of "OUT" resulted four orders of magnitude higher than the fluorescence values for "IN" (which was equal to the negative control). Therefore, we can conclude that the systems showed an optimal sealing ability with respect to external contaminants, an essential prerequisite in view of the target application.

These systems, developed to perform *in vitro* experiments, are based on the use of an ultra-thin polystyrene (PS) film (29 μm thickness, Goodfellow, Huntington, Cambridge, UK), also transparent to US, mounted within a CellCrown™ 24NX insert (Scaffdex, Tampere, Finland). The CellCrown™ had an open diameter of 8.6 mm and was

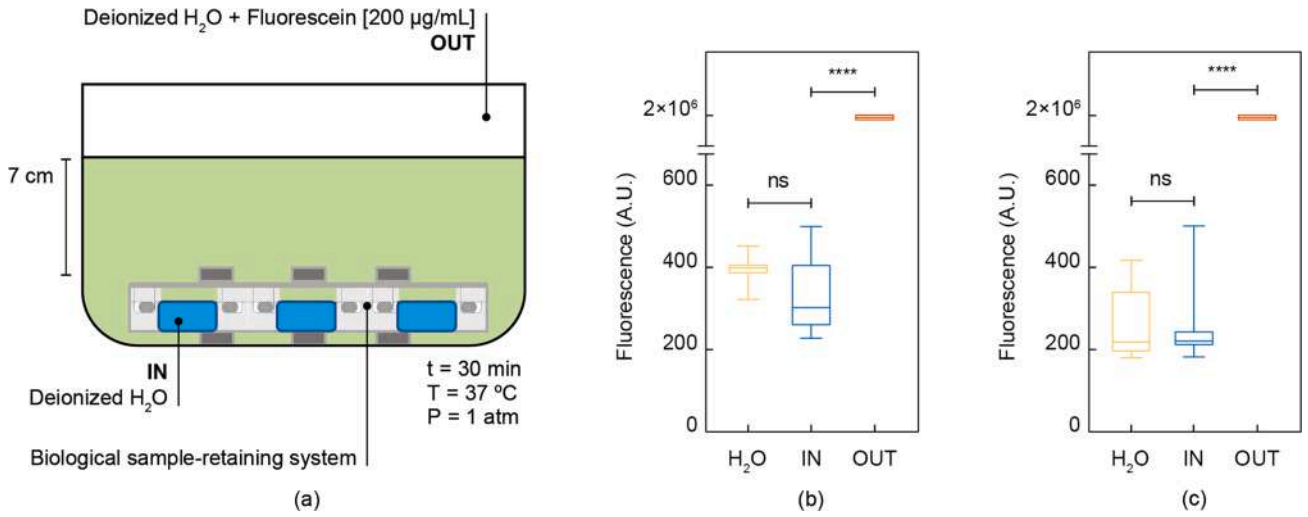

Fig. 5. Schematic representation of the impermeability test set-up (a) and impermeability test results for LFS (b) and HFS (c), in terms of fluorescence measurements: OUT represents the solution placed externally to the system (deionized water + 200 µg/mL fluorescein; IN represents the well content after 30 min incubation; H_2O represents the deionized water used as control. N = 12, Applied sealing torque = 20 N*m. ns = not significant, **** = $p < 0.0001$.

made of polycarbonate. Such insert could be easily inserted and removed from the chambers before and after US stimulation. This allowed keeping the biological samples (i.e. cells in monoculture or in 3D hydrogels) within standard cell culture supports (multi-well plates) for most of the time, maximizing the stimulation tool usability and minimizing possible contamination risks, as depicted in Fig. S5.

2.4. Microbiological analysis

A microbiological analysis was performed on both HFS and LFS systems to ascertain if they could be maintained uncontaminated even after extensive manipulations. Indeed, this aspect is a crucial one, when addressing relatively long stimulation experiments. This aspect was verified by including an additional element (a hydrogel) in the system, thus facing a worst-case condition, in which an additional element should be manipulated, in addition to the stimulation device. Each retaining system was manipulated four times/day (assembled and closed after each immersion in the water tank) for 7 days. A hydrogel (VitroGel, The Well Bioscience, North Brunswick, NJ, USA) was prepared as indicated by the manufacturer: 300 µL of the solution were poured on each ultra-thin PS film, mounted within a CellCrown™ 24NX insert, as previously reported. The hydrogels-loaded cell crowns were left to stabilize for 20 min at room temperature, transferred in a 24 well plate and 1.5 mL of culture medium was added to each of them. At the experimental time points (Day 1, 3 and 7) (Table SI), the inserts were transferred into the wells of HFS and LFS systems, filled with 3.5 mL of culture medium, covered with a PS membrane, as previously described and the assembled systems immersed in the water tank for 5 min. At the end of the fourth immersion of each experimental day (Table SI), the medium was collected from each well of HFS and LFS systems and transferred into new tubes to perform microbiological analyses. An aliquot of medium (100 µL) was directly spread on the plate using different non-selective media (Nutrient agar, Plate count agar, sheep blood agar) according to UNI EN ISO 6222:20016. All plates, in duplicate, were then incubated at 36 °C for 48 h to analyze the water environmental flora as well as the pathogenic bacteria able to grow at 36 °C in aerobic and anaerobic conditions, which could have affected the culture. At the end of the incubation time, the colonies were counted and results were expressed as colony formant units (CFU)/100 µL. The water filling the tanks (that was not changed for all the duration of the experiment) and swab samples performed on external o-rings, evidenced the presence of contaminants already at day 1. Therefore, to avoid the cross contaminations between the water tank and HFS and LFS during extensive manipulations in the water tank, the following tests were carried out adopting additional measures at each day/immersion: 1. use of sterile HFS or LFS; 2. use of new prepared re-filtered medium and sterilized disposable materials; 3. seal the top of the water tank with antimicrobial drape (3M, St Paul, MN, USA) at the end of each/day immersion.

The results reported in Table 1 showed the CFU/100 µL + SD of two different experiments and confirmed a low or null bacteria contamination in all the wells of both HFS and LFS as well as on the internal o-ring and the control medium. By contrast, high microbial contaminants were detected into the water tank that reached the external o-ring as shown by few colonies found on swab samples; the biochemical typing showed colonies belonging to common waterborne disease-related pathogens (i.e., Acinetobacter spp. and Citrobacter spp.) and typical nosocomial environmental microorganisms (i.e., Pseudomonas aeruginosa and Ralstonia pickettii).

The regularly changed medium (three times per week) in the HFS and LFS wells during the experiments, assured a continuous renewal of antibiotic treatment and fresh cell culture nutrients, so contributing to prevent contaminations.

Microbiological analyses were also performed on the Cellcrown™ inserts medium that, at the end of the experiment (Day 7), was still maintained for 21 days in the incubator at 37 °C, changing the medium twice a week. A low number of bacteria was counted, with absence of contaminations (until day 21), thus allowing to conclude that the basal bacterial contamination detected into the control medium and wells would have no impact on HFS- and LFS-based experiments also for

Table 1
Results of the microbiological analysis for environmental and pathogenic bacteria.

Samples	Day 1 Mean ± SD (cfu/100 µL)	Day 3 Mean ± SD (cfu/100 µL)	Day 7 Mean ± SD (cfu/100 µL)
Water filling the tank	19 ± 3	147 ± 11	292 ± 10
External O-ring	2 ± 2	2 ± 2	1 ± 1
Internal well O-ring	0	0	0
Control medium	2 ± 1	3 ± 1	4 ± 1
HFS medium from well 1	1 ± 2	1 ± 1	2 ± 1
HFS medium from well 2	2 ± 2	1 ± 2	1 ± 2
HFS medium from well 3	1 ± 2	0 ± 2	1 ± 2
LFS medium from well 1	1 ± 1	1 ± 2	1 ± 1

Results of the microbiological analysis for environmental and pathogenic bacteria, showed as colony formant unit (CFU)/100 µL ± SD of two different experiments.

longer time periods.

2.5. Acoustic simulations

Due to the impossibility to perform precise and accurate scanning measurements using the hydrophone within the biological sample-retaining system for encumbrance reasons, the US propagation within the set-up was simulated by using the k-Wave Matlab toolbox [27,28].

The simulation algorithm accuracy had been successfully validated by comparing the measured beam profiles and the simulated ones in free field conditions (Fig. 2a, b). A 2D approximated model of the main components of the retaining system was developed within the k-Wave environment, assigning the related acoustic properties to each different material. In Fig. S7, the model of the set-up, with its materials, is depicted; the corresponding acoustic properties are reported in Table SI.

As the CellCrown™ stretches the PS film on which cells will be seeded (Fig. 6a), the pressure distribution on the CellCrown™ PS film was computed for each frequency under investigation, and it is reported in Fig. 6b. In Fig. S8 the transverse distribution along the CellCrown™ diameter was also plotted for all the investigated frequencies, overlapping on the same graph curves deriving from the set-up case and from the free field case, in order to ease the comparison between them.

In order to quantify pressure homogeneity within the CellCrown™ film area, the mean absolute deviation (M.A.D.), expressed in (1) as percentage value, was computed (p_i represents the pressure value at a certain pixel point, μ is the spatial pressure average, and N is the total number of pixel points).

$$M.A.D. = \frac{\sum |p_i - \mu|}{N - 1} * 100 \quad (1)$$

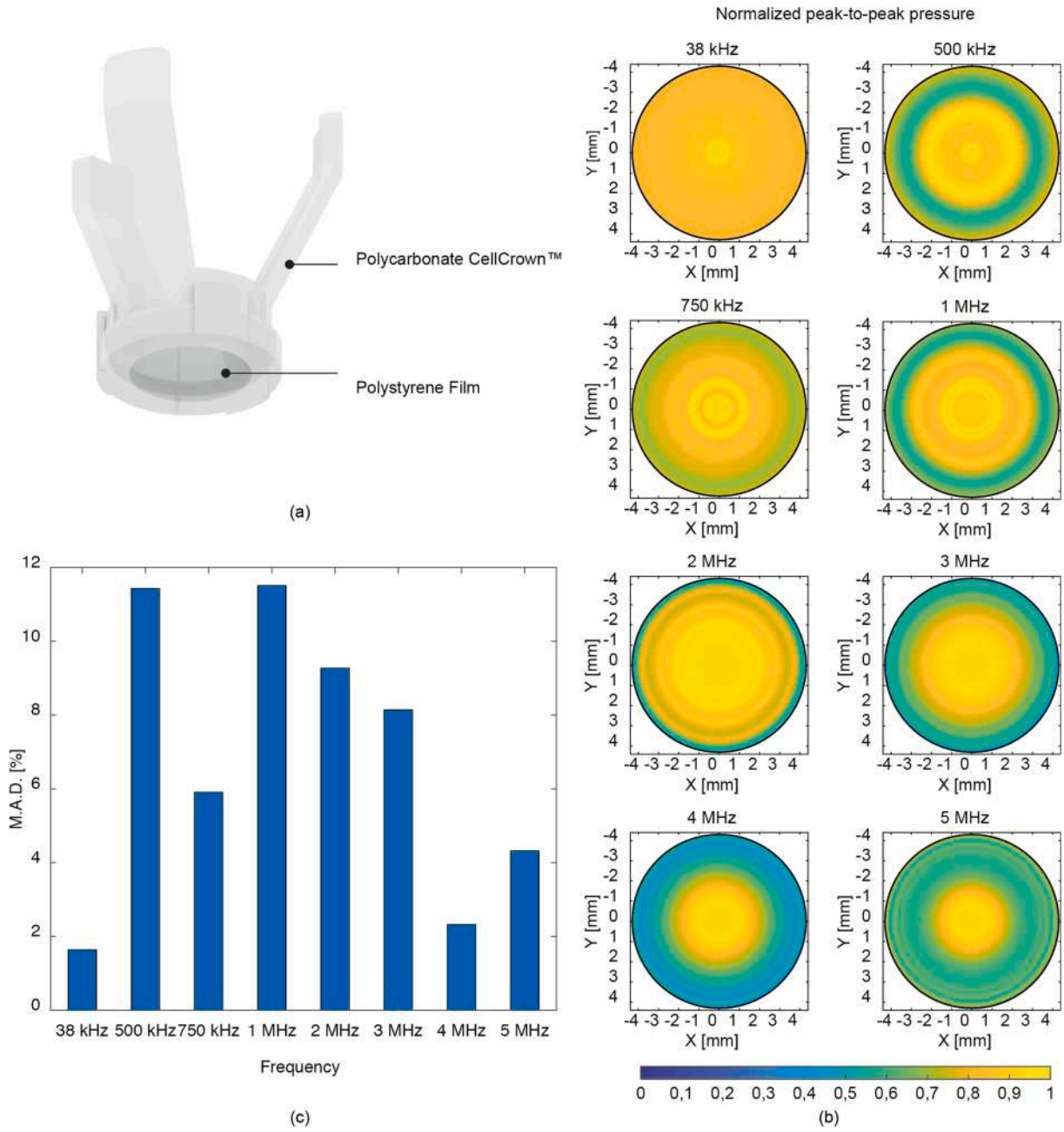

Fig. 6. (a) Rendered CAD of the polycarbonate CellCrown™, stretching the PS film. (b) Simulations results of the pressure distribution on the CellCrown™ PS film domain (the exact surface on which cells will be seeded): for each frequency, results are reported as normalized peak-to-peak pressure. (c) Bar graph of the mean absolute deviation (M.A.D.), as percentage value, for each frequency under investigation.

Results, reported in Fig. 6c, show a dispersion around the spatial average always lower than 11.5% (maximum value found at 1 MHz).

With the aim to estimate the real pressure which invests cells within the set-up, thanks to the simulation, the ratio between the spatial peak pressure in the "set-up" case and in the "free-field" case, within the CellCrown™ PS film domain, was then computed and it is reported in Table SII, for each frequency. An increment of the spatial peak pressure ratio is noticeable at lower frequencies, probably due to more significant diffraction phenomena, whereas a pronounced attenuation is shown at higher frequencies. It was anyhow possible in all cases to accurately estimate the US dose delivered at the target. In Fig. 7, the spatial average pressure values within the film that host cells, are reported for two representative experimental frequencies (38 kHz (a) and 1 MHz (b)), for both the set-up and the free field cases. The other graphs are reported in Fig. S9.

3. Biological validation

3.1. Cell adhesion and viability on the thin polystyrene film

Before culturing cells on it, the PS thin film was cleaned and sterilized under a biological safety cabinet class II by immersing the film for 2 h in sterile ethanol (EtOH) 70% (v/v) in sterile distilled water, rinsing it twice with sterile water, air-drying it, and then exposing it to ultraviolet (UV) light for 30 min. Squares (1.5 cm × 1.5 cm) were cut, inserted in CellCrown™ inserts and the excess material removed. The assembled CellCrown™ inserts were sterilized by exposing the top and the bottom face to UV light for 20 min each (Fig. S10). To verify cell adhesion on the PS film (0.58 cm^2 surface area), two cell lines were chosen: normal human dermal fibroblasts (nHDFs, Lonza, CC-2511), and Gibco™ Episomal human induced pluripotent stem cells (iPSCs, Gibco, A18945), representative of a rather delicate cell line. nHDFs were kept in culture in growth medium (GM), composed of high glucose Dulbecco's Modified Eagle Medium (DMEM, Sigma-Aldrich, cat. n° D6429), supplemented with 10% fetal bovine serum (v/v, FBS, Sigma-Aldrich, cat. n° F7524) and 100 IU/mL penicillin, 100 µg/mL streptomycin (Sigma-Aldrich, cat. n° P4333). The PS film was coated with fibronectin from bovine plasma (FN, 8 µg/cm^2, Sigma-Aldrich, cat. n° F4759) diluted in Dulbecco's phosphate buffered saline without Ca^{2+} and Mg^{2+} (PBS, Sigma-Aldrich, cat. n° D8537). Afterward, the PS film was left to air-dry for 45 min following the manufacturer's instructions and the remaining liquid was removed. CellCrown™ inserts were immersed in 1.45 mL of GM, 50 µL of the concentrated cell suspension was added (50,000 nHDFs/cm^2) and kept for 72 h in a CO_2 incubator (37 °C, 5% CO_2). A medium replacement at 48 h was performed. nHDFs growing on a FN-coated standard PS 24-well plate were used as control.

iPSCs were kept in culture on vitronectin-coated plates (VTN-N, 0.5 µg/cm^2, Gibco, cat. n° A14700) in stem cell growth medium (scGM), composed of Essential 8™ Flex Medium (Gibco, cat. n° A2858501) supplemented with 10 IU/mL penicillin, 10 µg/mL streptomycin. The PS film was coated with VTN-N (0.5 µg/cm^2) and left at room temperature for 1 h. Afterward, the remaining liquid was removed, CellCrown™ inserts were immersed in 1.45 mL of scGM, 50 µL of the concentrated cell suspension were added (10,000 iPSCs/cm^2) and kept for 72 h in a CO_2 incubator with a daily medium replacement. iPSCs growing on a VTN-N-coated standard PS 24-well plate were used as control.

Two samples for each condition were analyzed using a LIVE/DEAD® Viability/Cytotoxicity assay (Invitrogen) after 24 h, 48 h, and 72 h ("day 1", "day 2", "day 3"), without replacing the culture medium before the test. A Leica DMi8 microscope (Leica Microsystems, Wetzlar, Germany) was used for fluorescence image acquisition.

No significant differences were observed between the control and the cells cultured on the PS films, with a similar amount of dead cells (Fig. 8). These results indicate that the PS film did not raise cytotoxic effects, causing cell detachment or death, making it eligible for subsequent experiments in the HFS and LFS systems.

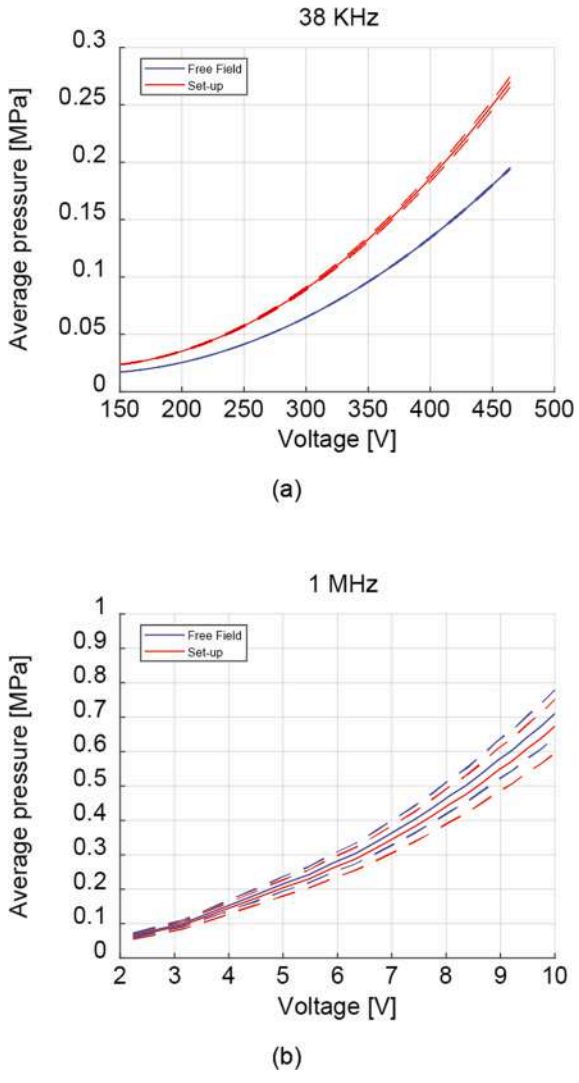

Fig. 7. Spatial average pressure values, aestimated within the film that hosts cells, for two representative frequencies (38 kHz and 1 MHz), for the set-up and the free field computed cases (curves are related to just one transducer for each frequency condition (Transducer 1)).

3.2. Sample sterility after immersion, evaluation of viability and metabolic activity on human adult primary chondrocytes, inflammatory activation of macrophages, and system functional evaluation

For the subsequent tests, both the HFS and LFS were used, performing mock tests simulating the conditions of immersion and sample manipulation typically occurring during US stimulation experiments. The two systems were sterilized by autoclaving the top and bottom polycarbonate disks and the hollow cylinders, and rinsing with EtOH 70% all the remaining components. Afterward, all the components were treated for 20 min with UV light. The PS film was cleaned and sterilized as described before. The latex film was cleaned and sterilized under a biological safety cabinet class II by washing it six times in distilled water. Each wash lasted 30 min and was performed in a US bath (frequency: 35 kHz). Afterward, the film was washed twice in sterile-filtered isopropanol 70% (v/v) for ten seconds each wash, without sonication. The film was then rinsed with distilled water, air-dried under the biological safety cabinet class II and exposed to UV light for 20 min. Squares (7 cm × 7 cm) were cut from the latex film and used in the sterile systems.

The average time needed by a non-skilled user to carefully insert three biological samples (with cells cultured on three CellCrown™

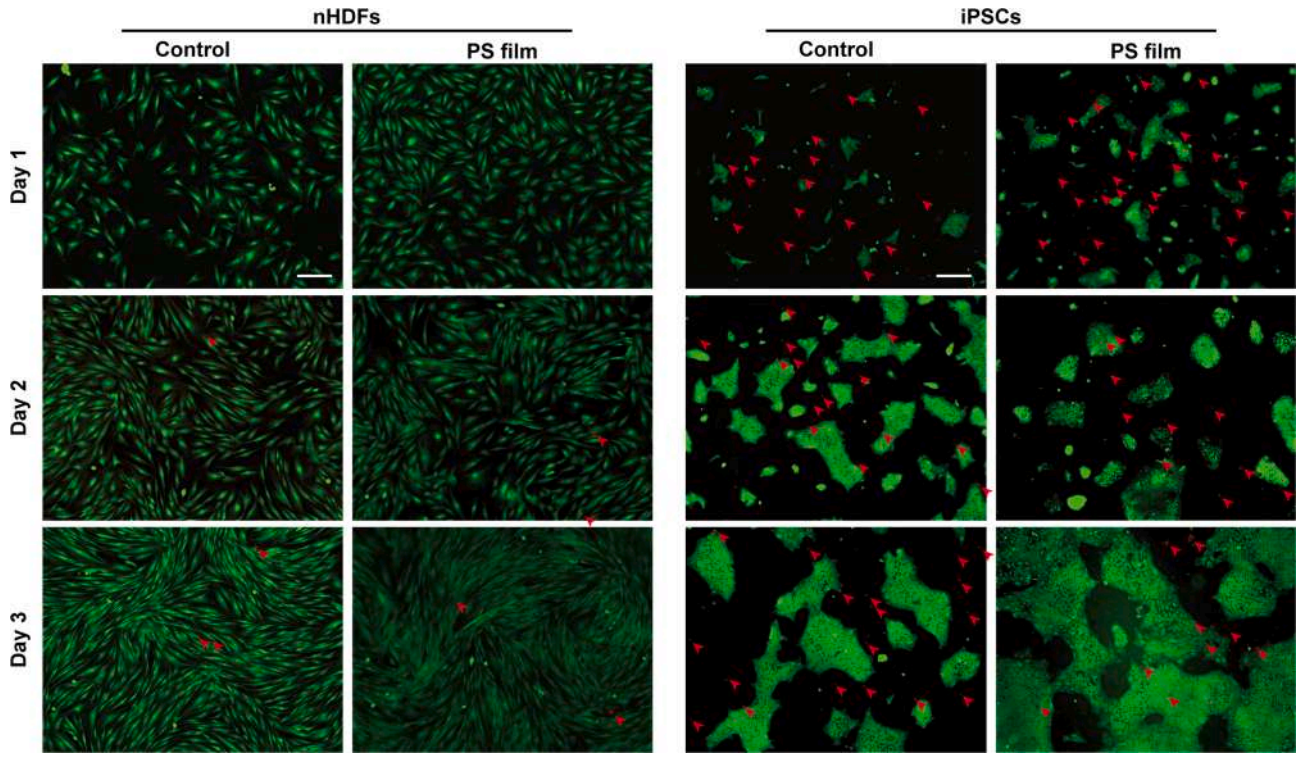

Fig. 8. Representative fluorescence images of adhesion and viability of normal human dermal fibroblasts and induced pluripotent stem cells on day 1, day 2 and day 3 post-seeding on the polystyrene films, compared to control. Green: viable cells; red: necrotic or dead cells, highlighted by red arrows. nHDFs = normal human dermal fibroblasts; iPSCs = induced pluripotent stem cells; PS = polystyrene. Scale bars: 200 μm.

inserts) in HFS, plus the system assembly and closure to make it ready for immersion in water, was ~9 min. Thus, being the HFS usable in triplicate, it means that ~3 min/sample were needed for preparing LIPUS stimulation experiments. Approximately 5 min were needed instead for the LIPUS stimulation experiments with LFS. ~1–2 min was needed to de-assembly the systems and remove the biological samples from the chamber, after the immersion.

CellCrown™ inserts were prepared as described before and human adult primary chondrocytes (haPCs, Cell applications, INC., 402-05a) were used for the tests on sample sterility, cell viability, and metabolic activity, while murine RAW 264.7 macrophage cell line (ATCC® TIB-71™) was used for evaluating the inflammatory activation. haPCs were kept in culture in chondrocyte growth medium (cGM, Cell applications, INC., cat. n° 411–500), while RAW 264.7 were cultured in GM. The complete experiment protocol is reported in Table SIII and Table SIV. Before cell seeding, CellCrown™ inserts were treated inside a plasma etching machine with oxygen plasma, to make the PS film more hydrophilic (Tucano Plasma RF 13.56 MHz, Gambetti. Parameters: 100% O_2, 50 s at 50 W and 0.5 mbar), UV-treated for 10 min, immersed in 1.45 mL of the appropriate culture medium and 50 μL of the concentrated cell suspension were added. Approximately 7,000 haPCs/cm^2 and 80,000 RAW 264.7/cm^2 were seeded separately in each sample. Oxygen plasma treatment was performed to ensure cell adhesion for the whole length of the experiment. DMEM was used in the culture system during immersions. In all the tests, during the system assembly, control samples (also cultured on CellCrown™ inserts) were kept in the same conditions of the HFS and LFS samples, namely at room temperature under a biological safety cabinet class II. Each immersion was performed in water at 37 °C and lasted 20 min, an interval included within the 30-min interval used during the impermeability tests. In parallel, control samples were kept in a standard PS 24-well plate at 37 °C. After the immersions, all samples (controls, HFS, and LFS) were transferred in a 24-well plate with fresh medium and kept in a CO_2 incubator.

Bacteria detection in the two systems was performed on haPCs 24 h after the first immersion (day 1). Microsart® ATMP Bacteria Patient kit (Sartorius) was used for this test, following the manufacturer's instructions. Briefly, 1 mL of the supernatant was taken from each sample without affecting the growing haPCs and then centrifuged for isolating possible bacteria. Bacterial DNA was extracted and a real-time polymerase chain reaction (qRT-PCR, RotorGene 6000, 2-plex HRM) was performed, amplifying a highly conserved region of the bacterial genome. The cycle threshold (Ct) of the samples was analyzed, setting the threshold line to 10% of the maximum fluorescence level of positive controls, as indicated in the protocol. The procedure correctness and the result were monitored thanks to the presence of a kit negative extraction control (NEC; if positive, DNA extraction failed), kit internal positive control (IPC; if negative, PCR amplification failed), and no-template control (NTC; if positive, buffers were contaminated by bacterial DNA). Results reported in Table 2 demonstrate that no bacterial DNA was found in all samples.

These data confirm the optimal sealing capability of the HFS and LFS in water, thus proving the two systems to be able to keep biological samples well isolated from the external environment.

After the assessment of contaminant absence in both systems,

Table 2
Result of the Bacterial Detection Analyses.

	Repl. 1	Repl. 2	NEC	IPC	NTC	Result
Ctrl	–	–	–	+	–	Bacteria
	Ct: 0	Ct: 0	Ct: 0	Ct: 21.45	Ct: 0	negative
HFS	–	–	–	+	–	Bacteria
	Ct: 0	Ct: 0	Ct: 0	Ct: 18.89	Ct: 0	negative
LFS	–	–	–	+	–	Bacteria
	Ct: 0	Ct: 0	Ct: 0	Ct: 17.04	Ct: 0	negative

Repl.: replicate; NEC: negative extraction control; IPC: internal positive control; NTC: no-template control; (−): absence of amplification; (+): presence of amplification; Ct: cycle threshold; Ctrl: control; HFS: high-frequency system; LFS: low-frequency system.

subsequent tests were performed to evaluate possible toxic effects on cells in the HFS and LFS.

Cell viability analyses were done on haPCs by using a LIVE/DEAD® Viability/Cytotoxicity Kit at day 1 and day 7, following the manufacturer's instructions. Two samples were analyzed for the control, data from all the samples of the HFS and LFS were collected. No medium replacement was done before the test. Representative images of control, HFS and LFS samples are shown in Fig. 9. No relevant differences were observed between control and samples from HFS and LFS: a higher number of dead cells can be observed after 7 days of culture in all the samples, most probably due to the high confluence reached by the cells. No correlation can be found between this behavior and the immersions with the HFS and LFS, since approximately the same amount of dead cells are observable in control samples too. Remarkably, no cell detachment was observed over a period of 7 days.

Quantitative analyses of cell viability and metabolic activity were performed on haPCs by using the PrestoBlue™ Cell Viability Reagent (Invitrogen) on day 1 and day 7, following the manufacturer's instructions. 1 mL of PrestoBlue™ Cell Viability Reagent was added to each sample and divided into 3 wells of 300 μL each for subsequent analyses. Data from day 1 to day 7 were collected on the same sample. The fluorescence signal at 560 nm was measured with a VICTOR Multilabel plate reader.

Three readings for each well were performed. Collected data are reported in Fig. 10 with boxes showing the median value, 25th and 75th quartile ± whiskers, ranging from the minimum to the maximum value.

Due to cell proliferation (see samples from day 1 to day 7 in Fig. 9) an increase in cell metabolic activity was observed between the same sample from day 1 to day 7 in all three conditions. Nevertheless, no relevant differences between control and HFS and LFS samples were detected.

Overall, data on haPC viability and metabolic activity suggest that repeated immersions of HFS and LFS in water over 7 days did not significantly affect cell viability and metabolic activity.

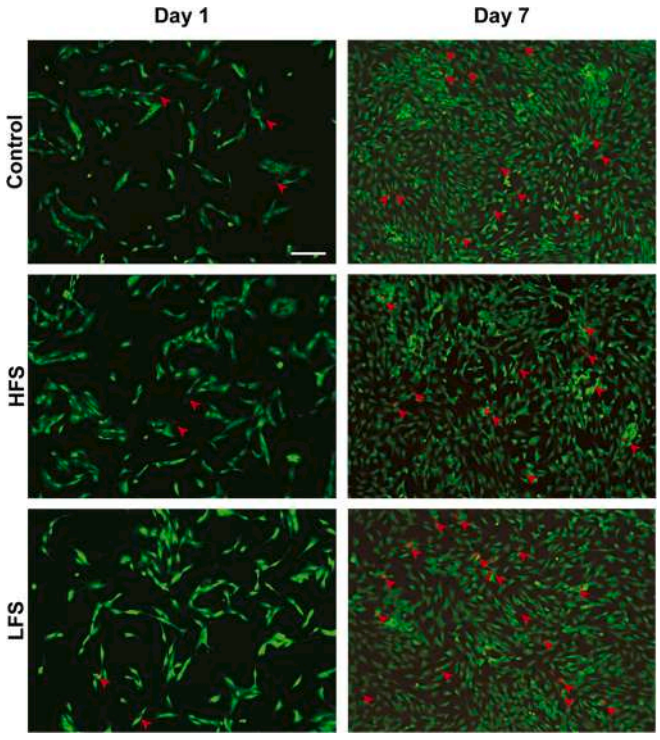

Fig. 9. Representative fluorescence images of human articular primary chondrocyte viability on day 1 and day 7 after multiple immersions, compared to control. Two images are shown for each sample. Green: viable cells; red: dead or necrotic cells, highlighted by red arrows. HFS = high-frequency system; LFS = low-frequency system. Scale bar: 200 μm.

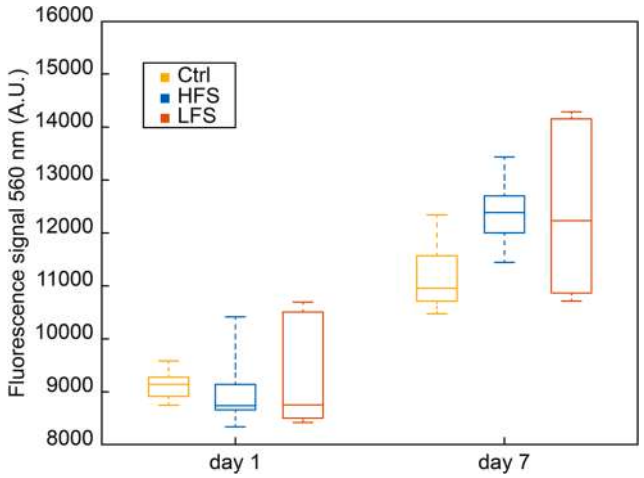

Fig. 10. Analysis of human adult primary chondrocyte metabolic activity on day 1 and day 7 after multiple immersions, compared to control. A.U.: arbitrary units; Ctrl: control; HFS: high-frequency system; LFS: low-frequency system.

In addition to possible cytotoxic effects caused by HFS and LFS, it is important to evaluate a hypothetical inflammatory response of cells. This information is relevant for the possible future *in vitro* studies on LIPUS anti-inflammatory effects on cells. It has been indeed demonstrated how LIPUS can interfere with the inflammatory response due to several molecular mechanisms still under investigation [13,30].

To this purpose, murine RAW 264.7 macrophage cells were seeded at day 0 as previously described (80,000 cells/cm^2). Immersion was done after 5 h, as reported in Table SIV. A positive control (also cultured on CellCrown™ inserts) was established by treating cells in a standard PS 24-well plate for 24 h with a solution of GM and lipopolysaccharides 1 μg/mL (LPS, from *Escherichia coli* 055:B5, Sigma-Aldrich), known to induce macrophage M1 pro-inflammatory state. Positive controls were treated like all the other controls, as already described before. Three samples were analyzed for the positive control; data from all the samples of the HFS and LFS were collected. All the samples were kept in the same medium volume (1.5 mL) until the analysis (day 1). Bright-field images were taken on day 1 to evaluate the inflammatory activation from morphological changes [31,32] (Fig. 11).

The intrinsic background of the PS film immersed in GM is shown in Fig. S11. No macrophage activation was observed in HFS and LFS samples, while several activated macrophages (round-shaped cells, flattened and bigger than non-activated ones) were observed in the positive control sample.

These data suggest that immersion of the biological sample retaining systems in water did not imply macrophage activation, thus not raising inflammatory phenomena.

After validating the two systems from a technological and biological point of view, the system was used to apply LIPUS stimulation on cells. A sonication experiment was performed on haPCs choosing three different frequencies (38 kHz, 1 MHz, and 5 MHz) and maintaining under very controlled conditions all the other parameters fixed: a spatial average pulse average intensity of 250 mW/cm^2, a duty-cycle of 20%; a pulse repetition frequency of 1 kHz and an exposure time of 10 min. Results are reported in the supplementary materials, section S1 and Fig. S12. Interestingly, the cells underwent different effects using 38 kHz, with respect to 1 and 5 MHz. Although the intensity was the same (and well controlled through the set-ups), by changing the frequency we modified the Mechanical Index (M.I.), defined in (2), indicating the ultrasound beam's ability to cause mechanical-related bioeffects.

$$M.I. = \frac{\max\{P_{neg}\}}{\sqrt{f}} \quad (2)$$

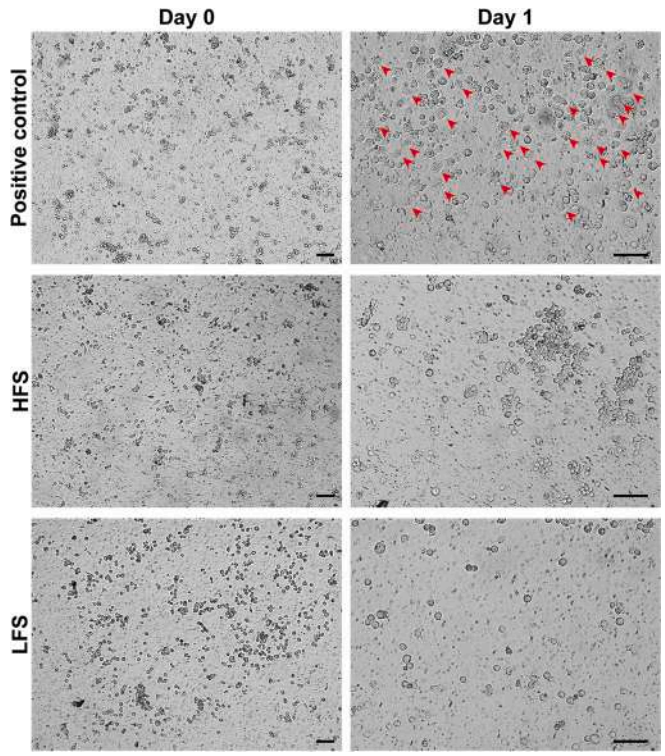

Fig. 11. Representative bright-field images of RAW 264.7 macrophages before the experiment (day 0, 5 h after seeding) and 24 h after the immersion (day 1). Activated macrophages are highlighted by red arrows. Positive control = lipopolysaccharides 1 μg/mL; HFS = high-frequency system; LFS = low-frequency system. Scale bars: 100 μm.

By sweeping the frequency from 5 MHz, to 38 kHz, the M.I. varied from a very low value (about 0.04 at 5 MHz), which was demonstrated to be within the safe ultrasound medical range [33], to a relatively high value (about 0.5 at 38 kHz), which is not always recommended in medical applications [34] and which caused in this experiment cell detachment

4. Discussion

The LIPUS set-ups here described are able to overcome several drawbacks affecting present state of the art systems. Marvel et al. [35] designed a custom *in vitro* LIPUS system, focusing on the control of the pulse repetition frequency parameter. Their attempt to accurately define the energy transmission resulted in a transducer calibration and an evaluation of the attenuation produced by an acoustically-transparent tissue culture film. Nevertheless, poor attention was paid to reflection phenomena due to sample exposure to air, which can hamper a precise amplitude delivery, due to significant acoustic impedance differences. The systems described in this paper were designed to prevent the issue of undesired wave reflections. This was achieved by completely immersing the biological sample-retaining system in water and inserting acoustic absorbers in the acoustic path. This required a careful design of the retaining system, which guaranteed sample impermeability to external contaminants, as demonstrated in Fig. 5b, c. As a consequence, this allowed to prevent bacterial infections (Table 2) and to guarantee a normal cell behavior, which was not altered by repeated immersions in water (Fig. 9, Fig. 10, Fig. 11).

Yddal et al. [36] fabricated a highly reproducible device to sonicate traditional 24-well culture plates and OptiCell™, using 3-D printing and low-cost consumables. In this case, even if a complete transducers calibration was carried out, the authors did not take care of the acoustic problems that could have affected the stimulation phase: the hard polystyrene culture plates were not meant to be acoustically transparent [35] and were exposed to open air, so producing reflection phenomena; at the same time, OptiCell™, and parallel plate chambers in general, can seriously compromise the efficacy of the stimulation tests in terms of cell viability-threatening procedures, besides the fact that they are disposable. In this work, as mentioned, we achieved good control of the transmitted US amplitude to cells, guaranteeing cell viability at the same time, by developing an easy-to-use, fast and non-disposable equipment (the only disposable parts are the CellCrown™ inserts, while all the other components are re-usable).

This represents a step forward also with respect to the work of Salgarella et al. [10]. Indeed, such a system guaranteed a single stimulation source, not allowing the user to stimulate multiple samples in parallel; further, a single engineered culture well took a relatively long time (~10 min/sample) to be assembled and disassembled and such a procedure implied an elaborated manipulation of the well components by the user, with a high risk of contamination and a consequent difficulty in carrying out long-term experiments. Furthermore, the culture well was not tested in terms of full sealing ability and sterility overtime.

The high-frequency system developed in this work can guarantee the simultaneous stimulation of three biological samples, with ~3 min/sample needed, for preparing LIPUS stimulation experiments. Further, it was proved that no contamination occurred during the experimental phase, even for several days, although the biological sample-retaining system was re-used for all tests.

Another significant added value for the herewith described systems, with respect to the state of the art, is the opportunity to modulate, with flexibility, a wide range of US parameters (frequency, intensity, duty-cycle, pulse repetition frequency) in order to process, in a controlled way, even US stimulation conditions that are very different from each other and from the previous ones explored up to now. This paves the way to the opportunity to discover new healing/regenerative effects on different cell and tissue types, in a precise and repeatable way.

5. Conclusion

This work describes the development and validation of two *in vitro* LIPUS stimulation systems. A full characterization was carried out, in terms of pressure field shape and intensity produced by transducers working in a wide range of frequencies, from 38 kHz to 5 MHz. 7 specific frequencies were investigated (500 kHz, 750 kHz, 1 MHz, 2 MHz, 3 MHz, 4 MHz, 5 MHz), but even intermediate frequencies of interest in this range could be analyzed in the future. The systems allowed a flexible adjustment of pulse repetition frequency and duty-cycle. Full control of the pressure amplitude at the target was possible, as demonstrated by acoustic simulations, performed on MATLAB acoustic toolbox k-wave. Such a system resulted at the same time US-controlled and impermeable to external contaminants, once immersed in water. In vitro tests confirmed the retaining system sterility after immersions. The thin polystyrene film used for culturing cells proved to support the culture of human fibroblasts and induced pluripotent stem cells. Experiments simulating the conditions of future LIPUS stimulation experiments demonstrated that multiple immersions of the systems over a period of seven days did not alter the viability and metabolic activity of human primary chondrocytes. In addition, no macrophage activation was observed.

Declaration of Competing Interest

The authors declare that they have no known competing financial interests or personal relationships that could have appeared to influence the work reported in this paper.

Acknowledgement

The authors acknowledge the European Union's Horizon 2020

research and innovation program grant agreement No 814414, ADMAIORA (ADvanced nanocomposite MAterIals fOr in situ treatment and ultRAsound-mediated management of osteoarthritis), and ImmUniverse project. ImmUniverse has received funding from the Innovative Medicines Initiative 2 Joint Undertaking (JU) under grant agreement No. 853995. The JU receives support from the European Union's Horizon 2020 research and innovation programme and EFPIA. The content provided in this paper reflects only the author's view and neither the IMI JU nor the European Commission are responsible for any use that may be made of the information it contains. The authors also acknowledge BAC s.r.l. for its contribution to the research activity.

Appendix A. Supplementary material

Supplementary data to this article can be found online at https://doi.org/10.1016/j.ultras.2021.106495.

References

[1] Z. Xin, et al., Clinical applications of low-intensity pulsed ultrasound and its potential role in urology, Transl. Androl. Urol. 2 (2016) 255–266.
[2] C. Ren, et al., LIPUS enhance elongation of neurites in rat cortical neurons through inhibition of GSK-3beta;1, Biomed. Environ. Sci. 23 (3) (2010) 244–249.
[3] L.B. Feril Jr., T. Kondo, Biological effects of low intensity ultrasound: the mechanism involved, and its implications on therapy and on biosafety of ultrasound, J. Radiat. Res. 45 (4) (2004) 479–489.
[4] A. Khanna, et al., The effects of LIPUS on soft-tissue healing: a review of literature, Br. Med. Bull. 89 (1) (2009) 169–182.
[5] Z. Izadifar, et al., Mechanical and biological effects of ultrasound: a review of present knowledge, Ultrasound Med. Biol. 43 (6) (2017) 1085–1104.
[6] S.-K. Castro-Luna et al., Evaluation of usability of two therapeutic ultrasound equipment, in: Proceedings of the 20th Congress of the International Ergonomics Association (IEA 2018), 2019, pp. 264–271.
[7] Y. Hu, et al., Ultrasound can modulate neuronal development: impact on neurite growth and cell body morphology, Ultrasound Med. Biol. 39 (5) (2013) 915–925.
[8] Y.W. Chen, et al., Therapeutic ultrasound suppresses neuropathic pain and upregulation of substance P and neurokinin-1 receptor in rats after peripheral nerve injury, Ultrasound Med. Biol. 41 (1) (2015) 143–150.
[9] Y.H. Tsuang, et al., Effects of low intensity pulsed ultrasound on rat schwann cells metabolism, Artif. Organs 35 (4) (2011) 373–383.
[10] A.R. Salgarella, et al., Optimal ultrasound exposure conditions for maximizing C2C12 muscle cell proliferation and differentiation, Ultrasound Med. Biol. 43 (7) (2017) 1452–1465.
[11] A. Katiyar, et al., Ultrasound stimulation increases proliferation of MC3T3-E1 preosteoblast-like cells, J. Ther. Ultrasound 2 (1) (2014) 1–10.
[12] N.N. Dedovich, et al., A device for low-frequency ultrasound therapy, Biomed. Eng. (NY) 51 (2) (2017) 138–141.
[13] E.M. da Silva Junior, et al., Modulating effect of low intensity pulsed ultrasound on the phenotype of inflammatory cells, Biomed. Pharmacother., Dec. 96 (2017) 1147–1153.
[14] K.H. Kim, et al., Low-intensity ultrasound attenuates paw edema formation and decreases vascular permeability induced by carrageenan injection in rats, J. Inflamm. (United Kingdom) 17 (1) (2020) 1–8.
[15] Y. Yue, et al., Low-intensity pulsed ultrasound upregulates pro-myelination indicators of Schwann cells enhanced by co-culture with adipose-derived stem cells, CellProlif. 49 (6) (2016) 720–728.
[16] C. Ren, et al., Low-intensity pulsed ultrasound promotes Schwann cell viability and proliferation via the GSK-3β/β-catenin signaling pathway, Int. J. Biol. Sci. 14 (5) (2018) 497–507.
[17] F. Dedola, et al., Ultrasound stimulations induce prolonged depolarization and fast action potentials in leech neurons, IEEE Open J. Eng. Med. Biol. 1 (January) (2020) 23–32.
[18] J.J. Leskinen, K. Hynynen, Study of factors affecting the magnitude and nature of ultrasound exposure with in vitro set-ups, Ultrasound Med. Biol. 38 (5) (May 2012) 777–794.
[19] S. Schimmel, Testing times Telling it like it is, vol. 95, 2005, pp. 12–13.
[20] A. Alassaf, et al., In vitro methods for evaluating therapeutic ultrasound exposures: present-day models and future innovations, J. Ther. Ultrasound 1 (1) (2013) 1–8.
[21] M. Snehota, et al., Therapeutic ultrasound experiments in vitro: review of factors influencing outcomes and reproducibility, Ultrasonics 107 (April) (2020) 106167.
[22] H. Tohmyoh, Y. Sakamoto, Determination of acoustic properties of thin polymer films utilizing the frequency dependence of the reflection coefficient of ultrasound, Rev. Sci. Instrum. 86 (11) (2015).
[23] L.M. Brekhovskikh, et al., Acoustics of layered media i: plane and quasi-plane waves (springer series on wave phenomena volume 5) second, updated printing (softcover); acoustics of layered media II: Point sources and bounded beams (Springer Series on Wave Phenomena Volume 10) Secon, J. Acoust. Soc. Am. 107 (4) (2000) 1809–1810.
[24] D. Ventre, et al., Enhanced total neurite outgrowth and secondary branching in dorsal root ganglion neurons elicited by low intensity pulsed ultrasound, J. Neural Eng. 15 (4) (2018) o.
[25] L. Zhao, et al., Low-intensity pulsed ultrasound enhances nerve growth factor-induced neurite outgrowth through mechanotransduction-mediated ERK1/2–CREB–Trx-1 signaling, Ultras. Med. Biol. 42 (12) (2016) 2914–2925.
[26] A. Cafarelli, et al., Tuning acoustic and mechanical properties of materials for ultrasound phantoms and smart substrates for cell cultures, Acta Biomater. 49 (Feb. 2017) 368–378.
[27] K. Firouzi, et al., A first-order k -space model for elastic wave propagation in heterogeneous media, J. Acoust. Soc. Am. 132 (3) (2012) 1271–1283.
[28] B.T. Cox, et al., k-space propagation models for acoustically heterogeneous media: application to biomedical photoacoustics, J. Acoust. Soc. Am. 121 (6) (2007) 3453.
[29] F. Fontana et al., Supporto per colture cellulari per stimolazione ultrasonica controllata. Italian patent application no. 102019000012696, Priority date: July 25, 2019.
[30] X. Zhang, et al., Inhibitory effect of low-intensity pulsed ultrasound on the expression of lipopolysaccharide-induced inflammatory factors in U937 cells, J. Ultras. Med. 36 (12) (2017) 2419–2429.
[31] J. Pi, et al., Detection of lipopolysaccharide induced inflammatory responses in RAW264.7 macrophages using atomic force microscope, Micron 65 (2014) 1–9.
[32] F.Y. McWhorter, et al., Modulation of macrophage phenotype by cell shape, Proc. Natl. Acad. Sci. U. S. A. 110 (43) (2013) 17253–17258.
[33] C.K. Holland, R.E. Apfel, Thresholds for transient cavitation produced by pulsed ultrasound in a controlled nuclei environment, J. Acoust. Soc. Am. 88 (5) (1990) 2059–2069.
[34] D.M. Rubin, et al., On the behaviour of living cells under the influence of ultrasound, Fluids 3 (4) (2018).
[35] S. Marvel, et al., The development and validation of a lipus system with preliminary observations of ultrasonic effects on human adult stem cells, IEEE Trans. Ultrason. Ferroelectr. Freq. Control 57 (9) (2010) 1977–1984.
[36] T. Yddal, S. Cochran, O.H. Gilja, M. Postema, S. Kotopoulis, Open-source, high-throughput ultrasound treatment chamber, Biomed. Tech. 60 (1) (2015) 77–87.